The discharge voltage behaviour during reactive sputtering of oxides

R. De Gryse, D. Depla, J. Haemers
Department of Solid State Sciences,
Ghent University, Krijgslaan 281 (S1), B-9000 Ghent, Belgium

ABSTRACT
The magnetron discharge voltage, measured in pure argon (or another noble gas) is characteristic for each kind of metallic targets. This discharge voltage is related to the Ion induced Secondary Electron Emission (ISEE) coefficient of the target material. In reactive sputtering a reaction gas is added to the sputter gas so that compounds (oxides, nitrides, carbides…) can be grown on a substrate. However, this reaction gas is also interacting with the target material forming also oxides, nitrides etc. In this paper we will limit ourselves to the situation in which the reaction gas is oxygen yielding oxides as well on the substrate as on the target surface. These oxides, formed on the target have a profound influence on the behaviour of the discharge voltage. Indeed, the higher the amount of oxygen added to the sputter gas (in this case only argon was used) the more oxide will be formed on the target surface and in the target subsurface region. In the limit, the target is fully plasma oxidised. This phenomenon gives rise to a change of the discharge voltage as a function of the oxygen flow, which is generally illustrated by the well known hysteresis experiments published in literature. As it is normally assumed that the ISEE of oxides is higher than the ISEE of the corresponding pure metallic targets, one expects a decrease of the discharge voltage upon the addition of oxygen to the sputter gas. The discharge voltage was measured for 15 different metallic target materials at constant current before and after plasma oxidation. Plasma oxidation of the target surface was achieved by sputtering the target in pure oxygen. It turned out that only 5 out of 15 target materials behaved “normal” i.e. displaying a lower target voltage when sputtering reactively as compared to metallic mode sputtering without oxygen.
Taking the Thornton relation into account, it is possible to establish a relation between the measured discharge voltage and published ISEE values for pure metals.
Based on this relation a value for the ISEE coefficient of the oxidized target surface can be calculated. Two distinct groups can be discerned: for one group the ISEE coefficient of the oxidized target surface is larger than the ISEE coefficient of the metal, while the opposite behaviour is noticed for the second group. This difference seems to find its origin in the reduction behaviour of the oxides under ion bombardment, since the ISEE coefficient of the oxide can be related to the simulated degree of reduction of the oxide. It is shown that the ISEE coefficient of the reduced oxides decreases with increasing oxygen content in the target. This is confirmed experimentally by sputtering in pure argon reduced titanium oxide targets with a known composition.

1. Introduction

Magnetron sputter deposition is a widely used physical vapour deposition technique to deposit thin films [1]. The sustaining process of the magnetron discharge is similar to a glow discharge. Indeed, ions are produced by ionisation of the discharge gas. These ions bombard the cathode which results in the emission of secondary electrons (Ion induced Secondary Electron Emission (ISEE)). The emitted electrons gain energy by acceleration over the sheath and can ionize the discharge gas. The magnetic field prevents the electrons from escaping the target (cathode) region before they produced a number of ions. Hence one refers sometimes to a magnetron discharge as a magnetically enhanced glow discharge.
During reactive magnetron sputtering from a metallic target, a reactive gas is added to the discharge to deposit compound material [2]. However, the addition of the reactive gas not only results in the formation of compound material on the substrate but also on the target surface where its formation is balanced by the sputtering process. The formation of the compound on the target changes its ISEE coefficient. This results, together with the modification of the plasma composition, in a change of the plasma impedance. If one keeps the discharge current constant, this change of the plasma impedance expresses itself in a discharge voltage change. Whether the voltage increases or decreases with regard to the discharge voltage in metallic mode depends on the target material [3]. This is also illustrated in figure 1, which compares the discharge voltage behaviour during oxygen addition/removal to an argon plasma during sputtering of titanium (figure 1a) and aluminium (figure 1b) under identical experimental conditions. The discharge voltage during reactive sputtering of aluminium decreases on oxygen addition in contrast to the case with a titanium target. As both the plasma composition and the target condition change when adding reactive gas to the vacuum chamber, it is difficult to distinguish between their influences on the discharge voltage measured at constant current. Moreover, values for the ISEE coefficient are not well documented in literature, especially for oxides or oxidized surfaces [4]. This hampers for example the simulation of the magnetron discharge since ISEE plays a key role in the sustaining process of the magnetron discharge [5].
Therefore, in this paper a method to study the influence of the target oxidation on the discharge voltage, irrespective of the plasma composition, is presented (see section 3.1.) The measured discharge voltage can be used to calculate the ISEE coefficient of the oxidized target surface by using the calibration line between the (inverse of) the discharge voltage and published ISEE coefficients for metal targets (see section 3.2.1 and 3.2.2). Further, the proposed method can be used to follow the sputter cleaning of the oxidized target surface, which allows calculating the sputter yield of the formed oxide material. The calculated sputter yields are compared with published sputter yields and simulated values using the software code SRIM [6] (see section 3.2.3). Based on the simulation some relationships between the

discharge voltage behaviour and the properties of the formed oxide are found. In this way, a better understanding of the material dependency of the discharge voltage changes during reactive sputtering can be achieved.

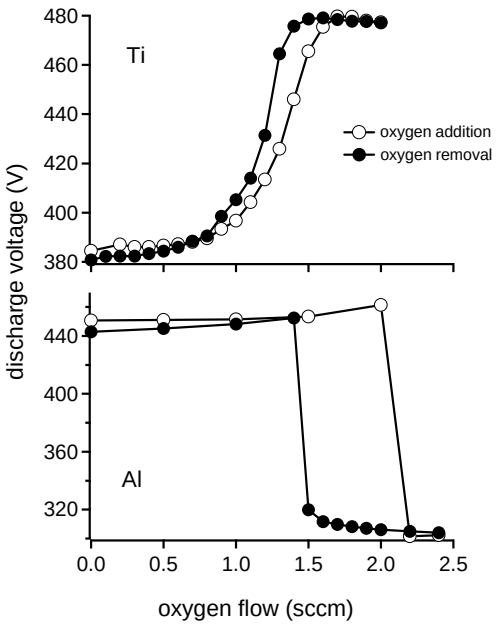

Figure 1. Discharge voltage behaviour during reactive sputtering of titanium and aluminium as a function of the oxygen flow (experimental conditions : constant current 0.4 A, constant Ar pressure: 0.4 Pa, pumping speed 65 L/s)

2. Experimental

The deposition chamber and the pumping equipment used for these experiments have been described in detail before [7]. Targets with a thickness of 3 mm, a diameter of 50.4 mm (2 inch) and a purity of 99.99% (Goodfellow (Ag, Au, Ta, Nb, Re, Ce, Pt, Y), and SCI Engineering materials (Mg, Al, Ti, Cr, Zr)) with a thickness of 3 mm and a purity of 99.99% were used in a conventional DC magnetron and powered with a DC generator (Hüttinger DC generator PFG 1500 W). Li targets were produced by cutting them from a 1.5 mm thick Li sheet (Alpha Aesar, 99.9% Li).

The used magnetron was described in detail in previous work [7] and its properties are similar as commercial available magnetrons. To test the influence of the magnetic field strength at the target surface, the target thickness was increased to 5 mm by inserting a 2mm copper plate between the target and the cathode surface, reducing the magnetic field strength parallel to the target surface to a value of 400 Gauss instead of 700 Gauss when using a 3 mm target. The magnet configuration results in a race track area of approximately 10 cm^2.

For a second set of experiments, targets produced by sintering a mixture of Ti and TiO_2 are used. A similar set of targets was used in a previous study where the effect of the target composition on the discharge voltage was studied [8][9]. All targets had a thickness of 3 mm. XRD has shown that TiO_2 and Ti react with each other, forming different compounds depending on the initial composition. Sintering the TiO_2 powder resulted in a non-stoichiometric target composition. Rutherford Back Scattering (RBS) showed that the actual composition was $TiO_{1.75}$. So, although the targets were composed initially from a mixture of TiO_2 and Ti the target can be better described as oxygen deficient TiO_{2-x} targets. Based on the XRD/RBS analysis it is possible to calculate the oxygen deficiency x in TiO_{2-x} (see table 1). As all targets had a resistivity lower than 0.7 Ωcm, the influence of the target impedance on the target voltage is negligible.

Table 1: Powder composition for the production of the titania targets

TiO_2 (wt. %)	Ti (wt. %)	Target phase composition	x in TiO_{2-x}
100	0	TiO_2 (rutile)	0.25
80	20	Ti_2O_3 (50%), TiO (50%)	0.6
65	35	TiO	1
50	50	TiO (small amount Ti_2O)	1.25
30	70	Ti_2O	1.6

When the DC voltage generator is switched on, a constant output voltage is obtained within its ramp time of 30 ms as mentioned in the manual and has been experimentally verified. According to the literature [10] it has been proven by optical emission spectroscopy during pulsed magnetron sputtering that within 40 µs a stable discharge voltage is obtained. Since we take into account only the voltages recorded 30 ms after switching on the power supply, the validity of the results can be trusted.

The discharge voltage was continuously measured during each experiment with a voltmeter and a computer system (sampling rate 1000 Hz). During the experiment the current was kept constant at 0.3 A (or 0.4 A). As Li has a low melting point (180°C)a lower discharge current (0.2 A) was used during the sputtering of Li.

3. Results and discussion

3.1. The oxidized target condition

To study the influence of the target oxidation on the discharge voltage, measured at constant current, the following experimental procedure was used for each target. First the target was sputter cleaned in pure argon until a constant discharge voltage was reached. We refer further in the text to this stable discharge voltage measured in argon at a constant current as V_{Ar}. Then, argon was replaced by, and the discharge voltage was measured in pure oxygen until a constant value was reached. We refer further in the text to this stable discharge voltage as V_{O2}. Afterwards the magnetron was switched off and the oxygen was replaced by argon. Once the sputter gas changed, the magnetron was switched on again while the discharge voltage was registered. The average time between the off-mode and the on-mode was approximately 5 seconds. We use the symbol $V_{ox,Ar}$ to refer to the initial discharge voltage measured 30 ms after the discharge was ignited in pure argon at constant current for a target which was first oxidized in pure oxygen. The complete procedure with used symbols is summarized in figure 2.

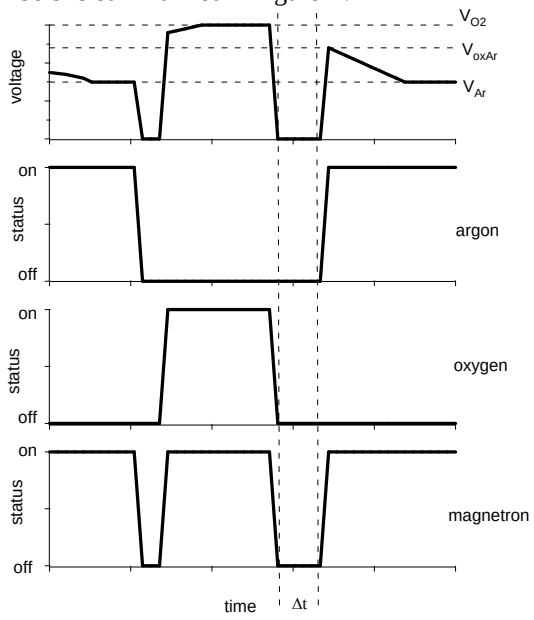

Figure 2. Schematic overview of the experimental procedure followed to study the influence of the target oxidation on the discharge voltage measured at constant current. Δt indicates the time interval between switching off the discharge in pure oxygen and the discharge ignition in pure argon.

Figure 3a shows the results for the studied metallic targets except for Li. The result for Li is shown in figure 3b, as a different discharge current was used. The discharge voltage returns during Ar sputtering from $V_{ox,Ar}$ to the value measured in metallic mode, i.e. V_{Ar}, as expected. For Al, Ce, Li, Mg and Y one notices that the discharge voltage on discharge ignition $V_{ox,Ar}$ is lower than the discharge voltage measured in metallic mode V_{Ar}. For the other studied materials an opposite behaviour is noticed, i.e. the discharge voltage on ignition $V_{ox,Ar}$ is higher than in the metallic mode V_{Ar}. Moreover, the discharge voltage behaviour in function of the argon sputter time is strongly material dependent, ranging from a quite simple behaviour (Ag, Al, Mg, Nb, Pt, Re, Ta and Y) to a complex behaviour (Au, Ce, Cr, Cu, Li, Ti and Zr). The origin of this complex behaviour is not understood yet and finds probably its origin in the formation and sputtering mechanism of the formed oxide layers on the target.

In the results presented in figure 3, the time interval Δt (see figure 2, for definition) between switching off the discharge in pure oxygen and the discharge ignition in pure argon was on average 5 seconds.

From previous experiments it follows that the measured discharge voltage $V_{ox,Ar}$ can depend on the time interval duration, an effect which has been attributed to e.g. oxygen atom diffusion, recombination and desorption as molecules from the surface [11][12]. Increasing the time interval between switching off the discharge in pure oxygen and switching on the discharge in pure argon (Δt see figure 2) from 5 seconds to 60 seconds did not alter the measured discharge voltage behaviour. So, the formed oxide seems to be stable in time.

3.2. Analysis of the experimental results

The experimental results shown in figure 3 contain information concerning the formed oxide layer during the plasma oxidation. Indeed, the discharge voltage is related to the ISEE coefficient of the oxide layer $ISEE_{ox}$. The time to return to the metallic state will depend on the sputter yield of the formed oxide layer Y_{ox}. Both values, i.e. the $ISEE_{ox}$ coefficient and the sputter yield Y_{ox} can be

Table 2: Overview of the experimental conditions during the oxidation of the metallic targets and the subsequent sputter cleaning in pure argon. Due to the low melting point of Li, the discharge current was set at 0.2 A during Li sputtering. By increasing the target thickness the magnet field strength is lowered (see experimental)

[2]Series	Constant current (A)	Constant Pressure (Pa)	Target thickness (mm)	Time interval duration Δt (s)
1	0.3	0.3	3	5
2	0.3	0.3	3	60
3	0.4	0.3	3	5
4	0.3	0.4	3	5
5	0.3	0.3	5	5

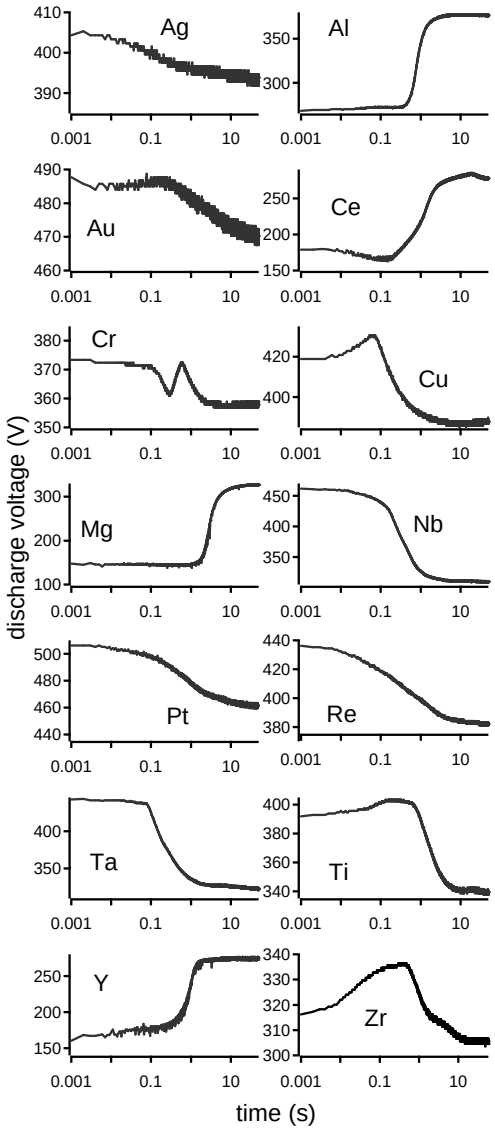

Figure 3a. Absolute value of the discharge voltage behaviour for oxidized targets sputtered in pure Ar, i.e. each plot shows the transition form $V_{ox,Ar}$ to V_{Ar} or stated differently the sputter removal of the formed oxide layer on the target surface. Experimental conditions see table 2, series 1

Figure 3b. Absolute value of the discharge voltage behaviour for an oxidized Li target sputtered in pure Ar. Experimental conditions 0.3 Pa Ar, 0.2 A. Target thickness 3 mm. Note that the scale of the x-axis is much larger than compared to figure 3a.

calculated from this type of experiments. However, to exclude the possible influence of the experimental conditions, i.e. the discharge current, the discharge pressure and the magnetic field, the experiments presented in figure 3, were repeated under different experimental conditions. An overview of them during oxidation of the target and the subsequent sputter cleaning in argon is given in table 2. The results of these experiments will be discussed in the following sections.

3.2.1. The metallic target condition

After sputter cleaning in pure argon, the target surface is in metallic state. In a previous paper [7] it was shown that the discharge voltage depends strongly on the target material.

The following equation was proposed by Thornton [13] for the minimum discharge voltage to sustain the magnetron discharge:

$$V_{min} = \frac{W_0}{\gamma \varepsilon_i \varepsilon_e} \qquad (1)$$

with W_0 the effective ionisation energy (about 30 eV for Ar^+, strictly speaking this value depends on the discharge voltage[32]), ε_i the ion collection efficiency, ε_e the fraction of the maximum number of ions V_{min}/W_0 that can be made on average by a primary electron before it is lost from the system and γ the effective secondary electron emission yield. Both ε_i and ε_e are close to unity for magnetron sputtering. The effective secondary electron emission yield γ is the product of the ion induced secondary electron emission (ISEE) coefficient γ_{ISEE} and the effective gas ionisation probability E [33]. Taking this into account, equation (1) gives :

$$V_{min} = \frac{W_0}{E(\ldots)\gamma_{ISEE}\varepsilon_i\varepsilon_e} \text{ or } \frac{1}{V_{min}} = E(\ldots)\frac{\varepsilon_i \varepsilon_e}{W_0}\gamma_{ISEE} \qquad (1')$$

If we assume a material independent recapture probability and keep the pressure constant, the factor E in equation (1') remains constant, which means that the inverse of the discharge voltage is proportional with the ISEE coefficient of the target material. This statement is irrespective of the discharge current as equation (1) is based on the conservation of energy. As shown by Phelps et al. [4] the ISEE coefficient depends strongly on the condition of the target material and on the ion energy. However, according to the same reference, the ISEE coefficient γ_{ISEE} for low ion energy (lower than 500 eV) and clean metal surfaces depends only on the potential energy of the ion. Several authors have published empirical relations for the ISEE coefficient in this energy regime:

[34]: $\gamma_{ISEE} = 0.032(E_i - 2\phi)$ (2)

[35]: $\gamma_{ISEE} = 0.016(E_i - 2\phi)$ (3)

[36]: $\gamma_{ISEE} = 0.017(E_i - 0.8\phi - E_F)$ (4)

with E_i the ionisation energy of the ion, ϕ the work function and E_F the Fermi energy of the metal. Based on these empirical relations, and published measured ISEE coefficients [7], an averaged value for the ISEE coefficient for each of the studied target materials was calculated.

As shown before [7] and repeated in figure 4, the measured discharge voltage for the metallic state, i.e. V_{Ar} is indeed inversely proportional to the $ISEE_M$ of the metal. The $ISEE_M$ coefficients are based on literature values and were taken from [7]. A straight line can be fitted to this data :

$$\frac{1}{V_{Ar}} = A + B \cdot ISEE_M \qquad (5)$$

Since the discharge voltage depends also strongly on the experimental conditions (discharge current, discharge pressure and magnetic field) the value of the intercept A and of the slope B will change. Hence, A and B are only valid for a given series of experiments (see table 2) during sputtering in pure argon.

3.2.2. The $ISEE_{ox}$ coefficient for the oxidized target surface

As discussed in the experimental part, the discharge voltage has been measured 30 ms after discharge ignition. The value of this discharge voltage ($V_{ox,Ar}$, see figure 2) can be compared directly with the value of the discharge voltage for the metallic target conditions (V_{Ar}, see figure 2) as both discharge voltages are measured under identical conditions in contrast to hysteresis experiments where the discharge voltage is also influenced by the plasma composition.

So, knowing the discharge voltage $V_{ox,Ar}$ one can calculate the $ISEE_{ox}$ using the equation of the fitted line derived in the previous paragraph (see equation 1)and presented in figure 4, i.e.

$$ISEE_{ox} = \frac{1}{B}\left(\frac{1}{V_{ox,Ar}} - A\right) \qquad (6)$$

with A the intercept and B the slope of the fitted line presented in figure 4 and equation (5).

This calculation was performed for each set of experiments (see table 2). Though the discharge voltage depends strongly on the experimental parameters, for both the metallic or oxidized target condition, we found no influence of the experimental conditions on the calculated $ISEE_{ox}$ coefficients. Therefore, we summarize the experimental values for the discharge voltages V_{Ar}, $V_{Ox,Ar}$ and V_{O2} in table 3, together with the calculated values for the $ISEE_{ox}$ coefficients averaged over the five series of experiments.

The literature data for the ISEE coefficient of oxides ($ISEE_{ox}$) in the ion energy regime of a few hundred eV is scarce due to the experimental difficulties to measure this data. For MgO a value of 0.2 is reported by Riccardi et al. [12] and Vogan et al. [14]. Although this is only half of the calculated value of $ISEE_{ox}$ for the oxidized Mg target surface (see table 3) reported here, it is still in the same order of magnitude. The applied calculation implicitly assumes that the

discharge voltage can be related to a change of the ISEE coefficient. Of course, another explanation could be based on a resistivity change of the target due to oxide formation. The influence of this effect will depend on the oxide thickness

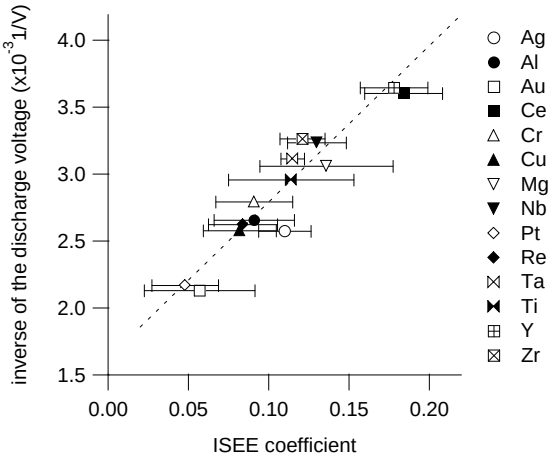

Figure 4. The inverse of the measured discharge voltage V_{Ar} in function of the ISEE coefficient $ISEE_M$ for different metallic target materials, measured at constant current (0.3 A) and constant argon pressure (0.3 Pa). The error bars are based on the minimum and maximum values reported in literature. The line is a linear fit with correlation coefficient r equal to 0.95 ($A=1.624x10^{-3}$ V^{-1} and $B=1.168x10^{-2}$ V^{-1}). The $ISEE_M$ coefficients are based on literature values and were taken from [7].

and the specific resistivity of the oxide. However, it is well known that Al_2O_3 has a high specific resistivity [15]. Even a thin layer of this oxide would result in a target resistivity increase, resulting in a discharge voltage increase at constant current. Nevertheless, a decrease of the discharge voltage is noticed. Moreover, it has been shown that the discharge voltage decreases on oxygen exposure, after the formation of the first monolayer by chemisorption. Indeed, when an aluminium target is exposed to an oxygen ambient without sputtering and subsequently sputtered in pure argon, a continuous decrease of the discharge voltage was noticed on increasing the exposure time [12][16].

Table 3: Discharge voltage of several target materials during series 1 (see table 2): V_{Ar} (discharge voltage measured in argon at constant current of 0.3 A and 0.3 Pa), V_{oxAr} (discharge voltage measured in argon at constant current of 0.3 A and constant argon pressure 0.3 Pa after oxidation of the target), V_{O2} (discharge voltage measured at constant current of 0.3 A in pure oxygen (0.3 Pa)). For the series 3, 4 and 5 (see table 2) the discharge voltage differs from the values reported in this table. The discharge voltage measured during sputtering of Li are measured at 0.2 A (*).
The ISEE coefficients of the metals $ISEE_M$ are based on literature data [7] The value between brackets is the calculated ISEE coefficient of the metal based on the fit presented in figure 4, using the discharge voltage value V_{Ar}. These latter values must be used to compare with the calculated value of the oxidized target surface $ISEE_{ox}$. The $ISEE_{ox}$ values are calculated as described in the text. The values are the average value of the calculated ISEE coefficients for the different experimental conditions as discussed in table 2. The error on the $ISEE_{ox}$ is in the order of 10%.

Target material	V_{Ar} (V)	$ISEE_M$	$V_{ox,Ar}$(V)	$ISEE_{ox}$	V_{O2} (V)
Ag	394.9	0.110 (0.081)	410.3	0.069	549.2
Al	376.4	0.091 (0.091)	259.1	0.198	305.8
Au	471.2	0.057 (0.047)	487.7	0.037	653.9
Ce	277.9	0.184 (0.17)	207.7	0.281	366.0
Cr	359.6	0.091 (0.102)	379.2	0.093	428.3
Cu	388.3	0.082 (0.084)	411.1	0.071	402.9
Li	299.6*	0.183*	299.8*	0.344*	353.6*
Mg	330.0	0.136 (0.123)	156.3	0.409	270.1
Nb	308.1	0.130 (0.141)	468.5	0.045	480.9
Pt	461.0	0.048 (0.05)	531.4	0.022	588.3
Re	379.7	0.084 (0.089)	482.0	0.039	616.8
Ta	321.1	0.115 (0.130)	435.3	0.058	431.9
Ti	335.6	0.114 (0.118)	391.9	0.080	428.6
Y	274.8	0.178 (0.173)	162.2	0.376	288.8
Zr	306.5	0.121 (0.142)	315.3	0.131	355.4

In conclusion, the noticed discharge voltage changes cannot be attributed to a change of the target resistivity but must be attributed to a change of the ISEE coefficient. Based on the relation between the $ISEE_M$ and the discharge voltage V_{Ar}, it is possible to calculate the $ISEE_{ox}$ using the measured value of the discharge voltage $V_{ox,Ar}$.

3.2.3. Oxide sputter yield

As shown before [17], it is possible to relate the argon sputter cleaning time of the oxidized target surface (see figure 3) to the sputter yield of the oxide material. Indeed, based on the experimental conditions during the plasma oxidation, one can estimate the oxide thickness. Following Todorov et al. [18] the oxide thickness formed during plasma oxidation can be estimated from the sum of the ion range and the straggle of the oxygen implanted during the plasma oxidation. Taking ½ eV_{O2} (see table 3) for the oxygen ion energy, the sum of the ion range and straggle was calculated using SRIM [6]. Half of the discharge voltage during plasma oxidation in pure oxygen, i.e. ½ V_{O2} was used because the molecular oxygen ions, formed by ionization of the oxygen molecules are accelerated over the dark space and will bombard the target with an energy almost equal to eV_{O2}. However, as the ion energy is much larger than the binding energy of the molecular ion, the molecular ion will break up on impact on the target in two oxygen atoms, each having about half of the energy of the original molecular oxygen ion.

Table 4: Calculation of the sputter cleaning time. Based on the sputter yield (literature values), the oxide layer thickness estimate from the sum of the ion range and straggle ($R_p + \Delta R_p$ calculated using SRIM), the sputter cleaning time was calculated. The experimental sputter cleaning time was measured from the discharge voltage behaviour during sputtering in pure Ar of the plasma oxidized targets (see figure 3).

Material	Total sputter yield $Y_{tot,ox}$ (published)	$R_p + \Delta R_p$ (nm)	Δt_{calc} (s)	Δt_{exp}(s)
Al_2O_3	0.25 [19]	1.5	0.392	0.347
Nb_2O_5	0.91 [19]	1.9	0.083	0.10
Ta_2O_5	1.25 [20]	1.9	0.064	0.078
Y_2O_3	0.28 [21]	1.8	0.234	0.206

Values for the sputter yield of oxides in the low energy regime (<500 eV) are not well documented in literature. To our knowledge this information has been published only for Al_2O_3 [19], Nb_2O_5 [19], Ta_2O_5 [20] and Y_2O_3 [21]. Based on this data, the validity of the calculation of the oxide layer thickness discussed in the previous paragraph can be tested [17]. Indeed, the erosion rate can be calculated using the published sputter yield and the oxide density together with the experimental value of the current density (0.03 A/cm^2). Dividing the oxide layer thickness, based on the SRIM simulations, by the erosion rate results in a calculated sputter cleaning time, which can be compared to the experimental sputter cleaning time (see figure 3). Table 4 summarizes the used sputter yields and the calculated results of the sputter cleaning time. The good agreement between the experimental and the calculated values confirms that the oxide layer thickness can be estimated from the sum of the ion range and straggle of the oxygen ions during reactive sputtering of the target in pure oxygen.

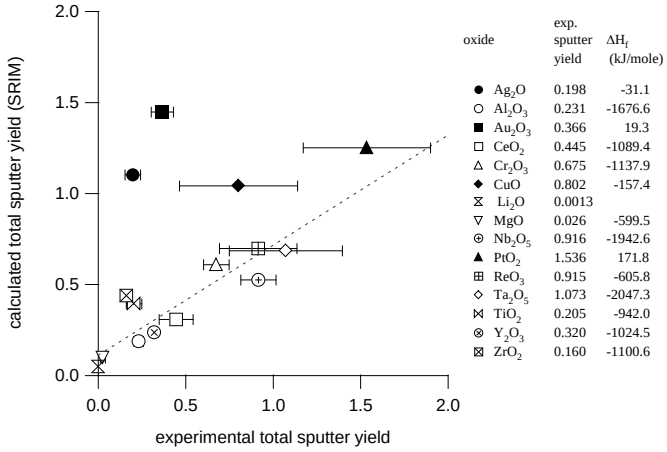

Figure 5. Correlation between the total sputter yield calculated using SRIM and the experimental total sputter yields for the oxides. The dotted line is a linear curve fit (r=0.85) between both sets with exception of the data for Ag, Au, Cu and Pt (full markers). The values for the experimental total sputter yield are given together with the heat of formation of the oxide (ΔH_f). The latter values were taken from [15][23][24]

Alternatively, based on this result, the sputter yield for the other oxides can be calculated from the results shown in figure 3. For each target material, the sputter cleaning time was measured from the spectra shown in figure 3. This was repeated for each series of experiments (see table 2). Also using SRIM, the ion range and the ion straggle was calculated using the same assumption on the ion energy as discussed above. Since the current density is known, the total sputter yield can be calculated as follows :

$$Y_{tot,ox} = \frac{(a+b)(R_p + \Delta R_p) N_a \rho_{ox}}{I_c / e \Delta t_{exp} (a MM_m + b MM_O)} \quad (7)$$

with a and b depending on the stiochiometry of the oxide M_aO_b, R_p and ΔR_p (cm) the ion range and straggle, I_c the experimental current density (0.03 A/cm^2), Δt_{exp} the sputter cleaning time (s), ρ_{ox} the density of the oxide with composition M_aO_b (g/cm^3), MM_m and MM_O, the molecular mass of the metal and oxygen (g/mole). N_a is Avogadro's number and e the elementary charge.

To test the validity of the experimental sputter yields, we have compared them with calculated sputter yields using SRIM. It is well known that the sputter yield depends strongly on the surface binding energy of the elements present in the target. In the case of oxides, several authors have proposed a model to calculate the surface binding energy of the metal and oxygen atoms in the oxide. In this work, the model of Malherbe et al. [22]has been used. The surface binding energy of the metal in this model is the heat of sublimation corrected with the electronegativity difference between the metal and the oxygen atom. The surface binding energy of the oxygen atoms depends on the metal-oxygen bond strength, the oxygen-oxygen bond strength and the electronegativity difference between the metal and the oxygen atom. All necessary values were taken from [15]. The surface binding energies calculated from the model of Malherbe et al. [22] were used, together with the oxide density and stoichiometry as input values in SRIM. When several oxides are possible, the oxide in which the metal has the highest oxidation state was chosen. The argon energy was set equal to $eV_{ox,Ar}$ (see table 3). Figure 5 summarizes the results. A linear relation between the experimental total sputter yield $Y_{tot,ox}$ and the sputter yield simulated using SRIM is found (dotted line). However for Ag, Au, Cu and Pt (full markers in figure 5) the correlation is bad. This is not surprising as the oxides of these metals are quite unstable as can be estimated when comparing their low or positive heat of formation with the heat of formation of the other oxides (see figure 5) As for these noble metals, the presence of the oxide and/or the calculation of their sputter yield are doubtful, we have excluded these elements from our analysis.

From the linear relationship between both sets of data, one can conclude that SRIM gives no absolute values for the sputter yield of the oxides but values which are proportional to the experimental sputter yields of the oxides.

In conclusion, during reactive sputtering an oxide layer with a thickness in the order of 1 to 2 nm is formed on the target surface. Based on the discharge voltage behaviour during sputtering cleaning of the oxidized target, it is possible to calculate the sputter yield of the formed oxide $Y_{tot,ox}$.

3.3. Material dependence of the ISEE coefficient

From the analysis above, it is clear that the plasma oxidation of the target surface strongly influences the ISEE coefficient. Moreover, two groups of materials can be distinguished. One where the ISEE coefficient of the target increases on oxidation (Al, Ce, Li, Mg,Y), and one where the ISEE coefficient decreases on oxidation (Cr, Nb, Re, Ta, Ti). For Zr the difference between the discharge voltage V_{Ar} and $V_{ox,Ar}$ is only 9 V, which makes a significant conclusion concerning the influence of the oxidation on the ISEE coefficient difficult. To understand the origin of this difference, we propose first a hypothesis based on literature data (see section 3.3.1). Then this hypothesis is experimentally verified by studying the discharge voltage behaviour of reduced TiO_2 targets (see table 1 and see section 3.3.2). Finally the calculated $ISEE_{ox}$ values are further interpreted based on the results of these latter experiments (see section 3.3.3).

3.3.1. Hypothesis

A compilation of ISEE data by Phelps et al. [4] for both clean and oxidized metal surfaces under Ar^+ bombardment shows that for oxidized target surfaces, the $ISEE_{ox}$ is larger than the $ISEE_M$ for clean metal surfaces when the Ar ion energies exceeds 180 eV. This confirms the general accepted idea that the ISEE coefficient for oxides is larger than for metals. Therefore, it is remarkable to state that after target oxidation, for a substantial group (Cr, Nb, Re, Ta, Ti and Zr) the ISEE coefficient decreases on oxidation. In contrast to the group (Al, Ce, Li, Mg, Y) for which the $ISEE_{ox}$ coefficient of the oxides is in the order of 0.3 and significantly larger than the $ISEE_M$ coefficient of the metals, the $ISEE_{ox}$ of the group (Cr, Nb, Re, Ta, Ti and Zr) is only in the same order of the $ISEE_M$ coefficient (0.1). A possible explanation of this discrepancy is based on the work of Wittmaack [25]. In this latter study, it is shown that the enhanced electron yield generated by the oxygen implantation in silicon is directly proportional to the fractional coverage of the surface with fully oxidized silicon, i.e. SiO_2. Suboxides (SiO_x with $x<2$) or isolated oxygen atoms embedded in Si, apparently produce only a negligible yield change. Wittmaack shows in the same study [25] that bombardment of the formed silicon oxide layer by neon ions results in a rapid decrease of the electron yield. This effect is attributed to the preferential loss of oxygen during the neon bombardment and the formation of suboxides. In conclusion it seems from this latter study that the ISEE coefficient of suboxides is much smaller than for oxides and should be in the same order of the ISEE coefficient of the metal.

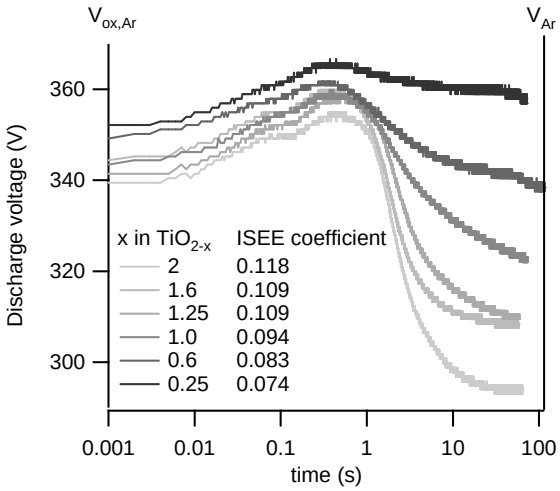

Figure 6. Discharge voltage behaviour after plasma oxidation of suboxide targets produced by sintering a mixture of TiO_2 and Ti (see table 1). Experimental conditions : argon pressure (0.5 Pa), constant current (0.12 A).

Based on this study, we propose the following hypothesis : the ISEE coefficient of the oxidized targets depends on the state of the formed oxide, i.e. a suboxide or an oxide. When a suboxide is formed, the ISEE coefficient is small and comparable to the ISEE coefficient of the metal. In contrast, if the target surface is fully oxidized, the $ISEE_{ox}$ coefficient is significantly larger than the $ISEE_M$ coefficient of the metal.
To test this hypothesis, one should first confirm the results of Wittmaack [25], i.e. suboxides have an ISEE coefficient comparable to the ISEE coefficient of the corresponding metal (see section 3.3.2). Secondly, one should determine the reason for the different behaviour of the two groups of metals on plasma oxidation (see section 3.3.3).

3.3.2. Sputtering of suboxides
To confirm the results by Wittmaack [25], the ISEE coefficients have been calculated for a set of titanium suboxides based on experiments published before [7]. The target composition is summarized in table 1. The experiments were performed in a similar way as described above. After plasma oxidation in pure oxygen, the targets were sputter cleaned in pure Ar.
Figure 6 shows the discharge voltage behaviour for the five targets, together with the discharge voltage behaviour of a Ti target sputtered under similar conditions. As discussed before, the discharge voltage behaviour is not related to the resistivity of the targets. Indeed, the measured resisitivity of the used titanium suboxide targets (<0.7 Ω.cm) is too small to explain the difference in discharge voltage. Moreover, as can be concluded from figure 6, after plasma oxidation the used targets have approximately the same discharge voltage $V_{ox,Ar}$ (between 340 and 350 V), indicating a similar target surface condition after plasma oxidation and a negligible influence of the resistivity.
The ISEE coefficient for these five suboxides was calculated based on the value of V_{Ar} (right axis, figure 6) using the same technique as discussed in paragraph 3.2.2, i.e a calibration line based on the $ISEE_M$ of metals, sputtered under identical conditions as the suboxides in argon (constant current 0.12 A and argon pressure 0.5 Pa : calibration line A = 1.77×10^{-3} (1/V) and B=1.12×10^{-2} (1/V), correlation r = 0.87) was used. As can be concluded from figure 6, the ISEE coefficient of all suboxide targets is smaller but in the same order than the ISEE coefficient of Ti, which confirms the first part of our hypothesis.

3.3.3. Material dependency of the $ISEE_{ox}$ coefficient
The target surface of the group (Al, Ce, Li, Mg and Y) has after plasma oxidation a high $ISEE_{ox}$ coefficient, while the opposite is found for the group (Cr, Nb, Re, Ta, Ti and Zr). Following our hypothesis plasma oxidation of the target surface of the first group should result in an oxide while for the latter group a suboxide will be formed. It is well known that an oxide can reduce under ion bombardment and a suboxide is formed [19]. The degree of reduction will depend on the balance between oxygen implantation and preferential sputtering of oxygen during plasma oxidation[26]. Moreover, during our experiments the surface is bombardment with argon ions during 30 ms before the discharge voltage $V_{ox,Ar}$ is recorded from which the ISEE coefficient is calculated.
This corresponds with an argon fluence of approximately 1×10^{16} ions/cm^2, which could also reduce the formed oxide. It is reported that Al_2O_3, CeO_2, MgO and Y_2O_3, i.e. the materials for which a high ISEE coefficient was measured, sputter congruently while most other oxides are sputter reduced [19][22][27][28]. So it seems that the two groups of materials can be distinguished based on the reduction behaviour under ion bombardment. This can be further confirmed by calculation of the reduction R of the oxide under argon ion bombardment using SRIM with the same settings as for the calculation of the sputter yields. The reduction R is defined as :

$$R = \frac{\left(M/O\right)^{s}}{\left(M/O\right)^{b}} \qquad (8)$$

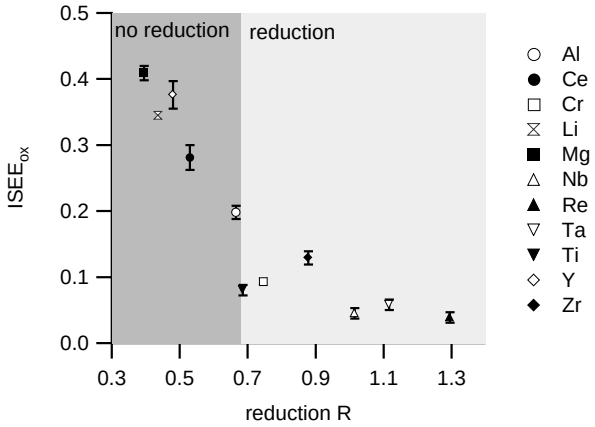

Figure 7. The influence of the reduction R (see equation 4) on the ISEE$_{ox}$ coefficient of the oxides. The reduction was calculated using SRIM. The noble elements (Ag, Au, Cu and Pt) have not been included as the SRIM calculation of the sputter yields (see figure 5) was not in agreement with the experimental results.

with M and O the mole fraction of the metal and oxygen at the surface (s) and in the bulk (b).
Figure 7 shows that a clear dependence of the ISEE$_{ox}$ on the reduction is found, further confirming the proposed hypothesis. Based on equation (8) one would expect the critical value to be 1. However, by comparison with published results for the reduction of oxides under ion bombardment [22][27][28], one can conclude that R = 0.66 (calculated with SRIM) seems to be a critical value, i.e. oxides with a value of R lower than the critical value are not reduced and have a high ISEE$_{ox}$, while the opposite is valid for oxides with a R value higher than the critical value. Hence, it seems that SRIM underestimate the exact value of R. Indeed, much higher values for the reduction R are found by Malherbe et al. [22]and Mitchell et al.[27]. An analogous conclusion as for the sputter yield calculation using SRIM can be drawn : a value proportional to the reduction is found using SRIM but the absolute value is not in agreement with the experimental results.
Based on the results of section 3.3.2 and 3.3.3 the discharge voltage behaviour during reactive magnetron sputtering can be understood from the formation of a thin layer which depending on the target material is a suboxide with a low ISEE$_{ox}$ or an oxide with a high ISEE$_{ox}$. The low ISEE$_{ox}$ for the suboxides is an interesting feature which needs further investigation as discussed in the following section.

3.3.4. Further analysis of the ISEE coefficient
The ISEE can be decomposed into the fraction due to potential emission and to kinetic emission [29]. In kinetic electron emission (KEE), electrons are excited as a consequence of the atomic motion of the projectile. In potential electron emission (PEE), electron excitation result from the conversion of the internal energy brought by the projectile, through an Auger process. At low energy (<400 eV) PEE is the major mechanism for secondary electron emission from clean metal surfaces. At the same energy the previously discussed compilation of ISEE data by Phelps et al. [4] shows that for oxides KEE is the major mechanism. It has been known for a long time that KEE for insulators is larger than for metals.
To understand KEE, one can divide the process into three steps : 1) production of primary electrons by ionization of target atoms by projectiles and by decay of plasmons excited by projectiles; 2) production of secondary electrons by fast primary and secondary electrons (cascade electrons), transport of electrons to the target surface; 3) escape of electrons with enough energy from the target surface.
As it is known that O atoms contribute less to the electronic yield than metal atoms[30], the production of primary and secondary electrons will decrease when the oxide layer contain more oxygen (step 1). Therefore, when comparing the ISEE$_{ox}$ of the suboxides, a lower ISEE$_{ox}$ can be expected when the bulk oxygen-to-metal ratio increases.
This seems to be confirmed as shown in Figure 8. This latter figure shows that the ISEE$_{ox}$ of the group with low ISEE$_{ox}$ (see figure 8, open markers) *and* the results for the TiO_x targets (see figure 8, star markers) can be related to the bulk oxygen-to-metal ratio using the *same* correlation line. Only the results for Zr deviates strongly from this line. So, although it seems from the SRIM simulations that ZrO_2 reduces (see figure 7), the measured ISEE coefficient is quite high. Indeed, the discharge voltage difference between V_{Ar} and $V_{ox,Ar}$ is only 9 V (see table 3).

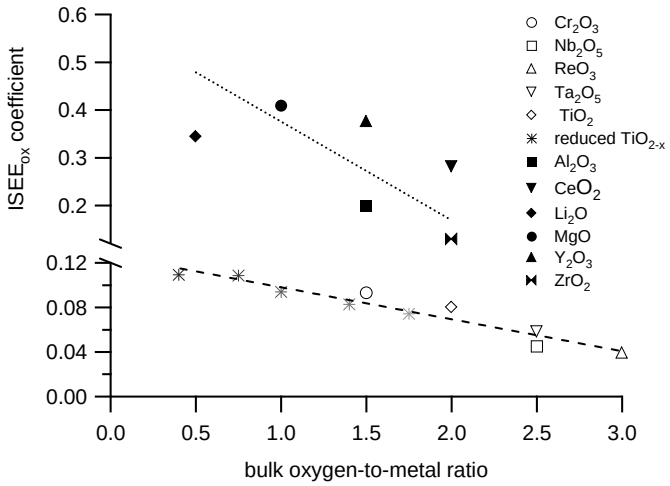

Figure 8. Relationship between the ISEE$_{ox}$ coefficient of the oxidized targets and the TiO_{2-x} targets and the bulk oxygen-to-metal ratio for oxides that reduce under ion bombardment and for oxides that not reduce under ion bombardment. Again the results for the noble metals (Ag, Au, Cu and Pt) have not been included as the SRIM calculation of their sputter yields (see figure 5) were not in agreement with the experimental results.

Hence, it is reasonable to add Zr to the group of oxides for which the ISEE coefficient increases. A similar relation between the ISEE$_{ox}$ coefficient and the bulk oxygen-to-metal ratio seems to hold for the fully oxidized, not reduced target surfaces (see figure 8, full markers). At first sight is seems surprising that the bulk oxygen-to-metal ratio influences the ISEE$_{ox}$ ratio. However, the reduction of the oxide will preferential occur at the surface but beneath this surface layer several authors [31]discuss the presence of a more oxidized layer, explaining the influence of the bulk oxygen-to-metal ratio.
As the ISEE$_{ox}$ coefficient of the suboxides is significantly lower than the ISEE$_{ox}$ than for the oxides, the preferential reduction of the surface layer probably lowers the escape probability of the electrons (step 3) and/or hampers the transport of the electrons to the target surface (step 2). The importance of the surface barrier on the ISEE coefficient has also been discussed in detail by Wittmaack [25].
In this way figure 8 summarizes our results. Depending on the type of oxide which is formed during plasma oxidation and subsequent sputtering in argon, the ISEE$_{ox}$ is high (oxide) or low (suboxide). The value of the ISEE$_{ox}$ depends on the bulk oxygen-to-metal ratio.

4. Conclusions

The discharge voltage behaviour during reactive magnetron sputter deposition of metal oxides finds its origin in the formation of an oxide layer on the target surface. Our experiments clearly show that this is not a monolayer as proposed in some models but is a layer in the order of 1-2 nm. The formation of this layer changes the ISEE coefficient of the target. Depending on the properties of the oxides under ion bombardment the ISEE coefficient of the target will increase or decrease. For oxides, which sputter congruently (Al_2O_3, CeO_2, MgO and Y_2O_3) the ISEE coefficient strongly increases in agreement with the general accepted idea that the ISEE coefficient of oxides is much larger than for metals. As a result, the discharge voltage measured at constant current will decrease as the plasma impedance is decreased. For oxides which reduce under ion bombardment, the ISEE coefficient is lower than the ISEE coefficient of the metal, which is confirmed by sputtering suboxide targets. However, the mechanism for this lowering is not been completely elucidated yet. Nevertheless, based on this study, we are able to distinguish between these two groups of metals.

References

[1] W.D.Westwood, 2003, Sputter Deposition (New York, AVS) ISBN 0-7354-0105-5
[2] S. Berg, T. Nyberg, Thin Solid Films 476 (2005) 215-230
[3] R. Mientus, K. Ellmer, Surf. Coatings Techn. 116-119 (1999) 1093-1101
[4] A.V. Phelps, Z.Lj. Petrovic, Plasma Source Sci. Technol. 8 (1999) R21-R44
[5] K. Nanbu, K. Mitsui, S. Kondo, J. Phys. D : Appl. Phys. 33 (2000) 2274-2283
[6] J.F. Ziegler, J.P. Biersack, L. Littmark (1985) The stopping and range of ions in Solids (New York, Pergamon). SRIM (Stopping and Range of Ions in Materials) can be downloaded from http://www.srim.org
[7] D. Depla, G. Buyle, J. Haemers, R. De Gryse, Surf. Coatings Techn. 200 (2006) 4329-4338
[8] D. Depla, H. Tomaszewski, G. Buyle, R. De Gryse, accepted for publication in Surf. Coatings Techn.
[9] H. Poelman, H. Tomaszewski, D. Poelman, D. Depla, R. De Gryse, Surf. Interface Anal. 36 (2004) 1167-1170
[10] J. Lopez, W. Zhu, A. Freilich, A. Belkind, K. Becker, J. Phys. D : Appl. Phys. 38 (2005) 1769-1780
[11] D. Depla, A. Colpaert, K. Eufinger, A. Segers, J. Haemers, R. De Gryse, Vacuum 66 (2002) 9-17
[12] D. Depla, R. De Gryse, Plasma Sources Sci. Techn. 10 (2001) 547-555
[13] P. Riccardi, M. Ishimot, P. Barone, R.A. Baragiola, Surf. Sci. 571 (2004) L305-L310
[14] W.S. Vogan, R.L. Champion, V.A. Esaulov, Surf. Sci. 538 (2003) 211-218

[15] CRC Handbook of Chemistry and Physics, 78th edition (1997) CRC Pres LLC
[16] D. Depla, R. De Gryse, J. Vac. Sci. Technol. 20 (2002) 521-525
[17] D. Depla, J. Haemers, R. De Gryse, accepted for publication in Thin Solid Films
[18] S.S. Todorov, E.R Fossum, Appl. Phys. Lett. 52 (1988) 48-50
[19] R. Behrish (ed.) Sputtering by Particle Bombardment II (1981), Springer-Verlag : Berlin, Heidelberg New York
[20] C.P. Hunt, M.P. Seah, Surf. Interface Anal. 5 (1983) 199-206
[21] S. Scaglione, L. Caneven, F. Sarto, J. Vac. Sci. Technol. A 12 (1994) 1523-1527
[22] J.B. Malherbe, S. Hofmann, J.M. Sanz, Appl. Surf. Sci. 27 (1986) 355-365
[23] Lange's Handbook of Chemistry (13th ed) (1985) edited by J.A. Dean, published by McGraw-Hill Inc, ISBN 0 0701 6192 5
[24] H. Tsai, E. Hu, K. Perng, M. Chen, J.-C. Wu, Y.-S. Chang, Surf. Sci. 537 (2003) L447-450
[25] K. Wittmaack, Surf. Sci. 419 (1999) 249-264
[26] S. Pétigny, H. Mostefa, B. Domenichini, E. Lesniewska, A. Steinbrunn, S. Bourgeois, Surf. Sci. (1998) 250-257
[27] D.F. Mitchell, G.I. Sproule, M.J. Graham, Surf. Interface Anal. 15 (1990) 487-497
[28] A.I. Zagorenko, V.I. Zaporzchenko, O.P. Ivanova, Surf. Interface Anal. 18(1992) 496-498
[29] R.A. Baragiola, Low Energy Ion-surface interactions, ed. J.W. Rabalais (1994) Wiley
[30] O. Benka, J. Pürstinger, Phys. Rev. A 58 (1998) 2978-2984
[31] C. Morant, J.M. Sanz, L. Galán, Phys. Rev. B 45 (1992) 1391-1398
[32] M.A. Lieberman, A.J. Lichtenberg, Principles of Plasma Discharges and Materials Processing, Wiley, New York, 1994, p. 81
[33] G. Buyle, W. De Bosscher, D. Depla, K. Eufinger, J. Haemers, R. De Gryse, Vacuum 70 (2003) 29
[34] R.A.Baragiola, E.V. Alonso, J. Ferron, A. Oliva-Florio, Surf. Sci. 90 (1979) 240
[35] Y.P. Raizer, Gas Discharge Physics, Spinger, New York, 1991
[36] L.M. Kishinevsky, Rad. Eff. 19 (1973) 23